Carbohydrate Polymers 87 (2012) 2648–2654

Contents lists available at SciVerse ScienceDirect

Carbohydrate Polymers

journal homepage: www.elsevier.com/locate/carbpol

Hydroxypropylcellulose templated synthesis of surfactant-free poly(acrylic acid) nanogels in aqueous media

Qian Liao, Qiaolan Shao, Haiyan Wang, Gao Qiu*, Xihua Lu*

State Key Laboratory for Modification of Chemical Fibers and Polymer Materials, College of Materials Science and Engineering, Donghua University, Shanghai 201620, PR China

ARTICLE INFO

Article history:
Received 8 July 2011
Received in revised form 1 September 2011
Accepted 14 November 2011
Available online 25 November 2011

Keywords:
Hydroxypropylcellulose
Acrylic acid
Hydrogen bonding
Temperature phase transition
Nanogels

ABSTRACT

We report the synthesis and study of surfactant-free poly(acrylic acid) (PAA) nanogels using hydroxypropylcellulose (HPC) as a template in aqueous HPC solutions at room temperature or above. Through the hydrogen bonding interaction of acrylic acid (AA) with hydroxypropylcellulose (HPC), AA absorbed on the HPC polymer chains and triggered the phase transition of HPC at a lower temperature, with increasing AA concentration, than the HPC intrinsic phase transition temperature 41 °C. As AA polymerized to form PAA, the much stronger interpolymer hydrogen bonding triggered the phase transition of HPC at a temperature around room temperature, causing HPC coil-global phase transition to collapse and form nanospheres at room temperature, PAA hydrogen-bonded HPC chains collapsed and formed nanogels chemically crosslinked by poly(ethylene glycol) diacrylate (PEGDA) or methylenebisacrylamide (BIS). The results showed that all the PAA nanogels demonstrated a narrow size distribution with diameters ranging from 60 nm to 600 nm.

1. Introduction

In recent decades, nanogels, *i.e.*, hydrogel nanoparticles with diameters in the range of tens to hundreds of nanometers, have attracted interest because of their significant importance in fundamental studies and practical applications (Hu, Tong, & Lyon, 2010; Kim, Singh, & Lyon, 2006; Lu, Hu, & Gao, 2000; Peer et al., 2007; Scherzinger, Lindner, Keerl, & Richtering, 2010). Due to their small size, stimuli-responsive nanogels can show a much more rapid (almost instantaneous) response to microenvironmental stimuli such as temperature and pH, compared with bulk hydrogels (Wang, Gan, Lyon, & El-Sayed, 2001). Polymeric nanogels are being developed for applications in cancer diagnosis and therapy, DNA and protein separation, tissue engineering, and biosensors (Khemtong, Kessinger, & Gao, 2009; Tabuchi et al., 2004; Xu, Goponenko, & Asher, 2008).

Emulsion precipitation polymerization and inverse emulsion polymerization have been developed for the synthesis of numerous nanogels (Kriwet, Walter, & Kissel, 1998; Pelton, 2000). Emulsion precipitation polymerization for the preparation of thermosensitive poly(N-isopropylacrylamide) (PNIPA) nanogels was first reported by Pelton's group early in 1986 (Pelton & Chibante, 1986). In this method, the PNIPA polymer chains collapse to form nanoparticles in an aqueous media at a high temperature well above the phase transition temperature of the PNIPA polymer. But emulsion precipitation polymerization is only utilized to synthesize thermosensitive polymer-based nanogels. For hydrophilic polymer nanogels without thermo-sensitivity, the polymer chains comprising the nanogels do not usually collapse to form nanoparticles in aqueous media. Thus, an alternative method, inverse emulsion polymerization, has been employed to synthesize different kinds of numerous hydrophilic nanogels such as poly(acrylic acid) (PAA) and poly(methacrylic acid) (PMAA) nanogels. Poly(acrylic acid) (PAA) is FDA-approved, pH-sensitive polymer for application in a wide variety of household and personal care products such as diapers, toothpastes, and hand sanitizers. PAA nanogels have found many potential applications in controlled drug release, nanotechnology for diagnosis and therapy, and bioadhesive products (Lee et al., 2007; Wu, Shen, Banerjee, & Zhou, 2010; Yu et al., 2008). Usually, PAA nanogels are synthesized by inverse emulsion polymerization. However, the inverse emulsion polymerization system contains a large amount of organic solvent and emulsifier which are not only harmful to the environment, but difficult to be completely removed from the nanogel dispersions. Such nanogels synthesized via inverse emulsion polymerization are difficult to develop for in vivo applications in humans.

Hydroxypropylcellulose (HPC) is a naturally derived carbohydrate polymer, which exhibits a phase transition around 41 °C in aqueous media (Chang & Zhang, 2011; Uraki, Imura, Kishimoto, & Ubukata, 2004). In this study, our group systematically studied HPC-templated synthesis of surfactant-free PAA nanogels through the variation of HPC and AA concentrations, crosslinker types and

* Corresponding authors. Tel.: +86 21 6779 2401; fax: +86 21 6779 2199.
E-mail addresses: gqiu@dhu.edu.cn (G. Qiu), xhlu2002@gmail.com (X. Lu).

0144-8617/$ – see front matter © 2011 Elsevier Ltd. All rights reserved.
doi:10.1016/j.carbpol.2011.11.056

their concentrations, and pH value. Our work showed why the water-soluble monomer AA can polymerize to form PAA nanogels in aqueous media using HPC as a template. First, the monomer AA attaches to the HPC polymer chains through the hydrogen bonding in the HPC/AA aqueous solution. Then, as AA polymerizes to form PAA, the interpolymer hydrogen bonding between HPC and PAA reduced the phase transition temperature of HPC to occur at a lower temperature or even around room temperature. Above the lower critical solution temperature (LCST), HPC (Lu, Hu, & Schwartz, 2002; Yao, Xu, Lu, & Deng, 2011) chains dehydrated to form nanoparticles, and then PAA chains attached to HPC collapsed to form PAA nanogels following the formation of the HPC nanogels. The resulting PAA nanogels maintained a very small size and narrow polydipersity, and were colloidally stable at pH (6.3 ± 0.3). A relatively high density of reactive COO^- groups in PAA nanogels may enable functionalization for the encapsulation of other nano materials (Zhang, Xu, & Kumacheva, 2004).

2. Experimental

2.1. Materials and methods

Hydroxypropylcellulose (HPC) powders (average $M_w = 1.0 \times 10^5$), acrylic acid monomers (AA, 99%), N,N′-methylenebisacrylamide (BIS, crosslinker, 99%), poly(ethylene glycol) diacrylate (PEGDA, $M_w = 258$), poly(ethylene glycol) diacrylate (PEGDA, $M_w = 700$), ammonium persulfate (APS, 99%, initiator), N,N,N′,N′-tetramethylethylenediamine (TEMED) were all purchased from Sigma–Aldrich Chemical Co. and used as received. Sodium hydroxide (NaOH) was supplied by Sinopharm Chemical Reagent Co., Ltd.

2.2. UV spectroscopy characterization of phase transition of 0.1 wt% HPC solution induced by different AA concentrations

0.5 wt% HPC water solution was prepared by dissolving HPC powder in deionized water under gentle stirring for 3–4 days at room temperature. 0.1 wt% HPC aqueous solutions with different AA concentrations of 0 wt%, 0.5 wt%, 1 wt%, 2 wt%, 5 wt%, and 10 wt% were prepared from 0.5 wt% HPC solution and 99 wt% AA. These solutions were measured at a heating rate of 0.2 °C/min by means of Lambda 35 UV–vis spectroscopy (Perkin Elmer, USA), respectively.

2.3. Preparation of PAA nanogels

1 wt% HPC water solution was prepared by dissolving HPC powder in deionized water under gentle stirring for 3–4 days at room temperature. PAA nanogels were prepared as follows: 40 g of 1 wt% HPC, 0.4 g AA, 0.3 g crosslinking agent BIS and 0.1 g APS were added into 59.1 g of deionized (DI) water with stirring to make a homogenous solution; the solution was purged with nitrogen for 40 min and heated up to 26 °C, at which time 0.1 g of TEMED was added to initialize polymerization of PAA, which was then allowed to proceed for 1 h. The resulting PAA nanogels were dialyzed against the unreacted AA, BIS, and TEMED for 3 days. And the aqueous dispersion of the PAA nanogels was neutralized to pH = (6.3 ± 0.3) by NaOH.

2.4. Dynamic light scattering (DLS)

The size and size distribution of PAA nanogel (1.2×10^{-5} g/ml) dispersions were measured by dynamic light scattering with a BI-9000 AT digital time correlator (BI-200SM, Brookhaven CO., Ltd.) at pH = 6.3 and 25 °C at a scattering angle of 90°. The light source was a He–Ne laser (35 mW and 633 nm). For dynamic laser light scattering (LLS), with the self-beating mode, the intensity–intensity time correlation function $G^{(2)}(t, q)$ was measured and can be expressed by (Chu, 1991)

$$G^{(2)}(t, q) = \langle I(t, q)I(q, 0)\rangle = \langle I(0)\rangle^2 g^{(2)}(t) = \langle I(0)\rangle^2[1 + |g(1)(t)|^2] \quad (1)$$

where t is the decay time and $q = (4\pi n/\lambda_0)\sin(\theta/2)$. $g^{(1)}(t) \equiv [\langle E(0)\, E^*(t)\rangle / \langle E(0)\, E^*(0)\rangle]$ and $g^{(2)}(t) \equiv [\langle I(0)\, I(t)\rangle / \langle I(0)\rangle^2]$ are the normalized field-field and normalized intensity–intensity autocorrelation functions, respectively.

In practice, the detection area cannot be zero. Therefore, to take into account deviations from ideal correlation, the function $g^{(1)}(q, t)$ is related to the line-width distribution $G(\Gamma)$ by

$$g^{(1)}(t, q) = \int_0^\infty G(\Gamma) e^{-\Gamma t}\, d\Gamma$$

$G(\Gamma)$ can be obtained from the Laplace inversion of $g^{(1)}(q, t)$, analyzed by a cumulant analysis to get the average line width $\langle\Gamma\rangle$ and the relative distribution width $\mu_2/\langle\Gamma\rangle^2$ with $\mu_2 = \int_0^\infty (\Gamma - \langle\Gamma\rangle)^2 G(\Gamma)\, d\Gamma$. The value of $\mu_2/\langle\Gamma\rangle^2$ provides a measure of the polydispersity index (PDI) of a given sample, and is given by the ratio of the standard deviation to the average hydrodynamic radius in a Gaussian size distribution. $G(\Gamma)$ can be converted to the translational diffusion coefficient distribution $G(D)$ and to the hydrodynamic diameter distribution $f(D_h)$ using the Stokes–Einstein equation:

$$D_h = \frac{k_B T}{3\pi\eta D}$$

Here k_B, T, and η are the Boltzmann constant, the absolute temperature, and the solvent viscosity, respectively.

2.5. Fourier transform infrared (FTIR) spectroscopy

The freeze-dried samples (2 mg) of nanogels, PAA, and HPC powders were each ground with KBr. The FTIR spectra were recorded by means of a Fourier transform spectrometer (NEXUS-670, Nicolet CO., Ltd.) running at a 4 cm^{-1} resolution.

2.6. Transmission electron microscopy (TEM)

The TEM micrographs of the air-dried samples were taken with a Hitachi CO. H-800 at an accelerating voltage of 200 kV.

2.7. Atomic force microscopy (AFM)

All AFM experiments were performed with a NanoScope IV SPE system (Veeco, USA) using a large multipurpose scanner (maximum scan range approximately 125 μm × 125 μm and vertical 2.5 μm).

3. Results and discussion

3.1. Acrylic acid-induced phase transition of aqueous hydroxypropylcellulose (HPC) solution

PAA nanogels were prepared in a conventional way, *i.e.*, via inverse emulsion polymerization as the water phase containing PAA dispersed in continuous oil phase with emulsifier (Landfester, Willert, & Antonietti, 2000). In this method large quantities of organic solvent and surfactant were used, resulting in environmental and toxicity issues. To eliminate the adverse effect of organic solvent and surfactant or emulsifier, we developed the synthesis of surfactant-free PAA nanogels directly in a HPC aqueous solution, a "green" method. One may wonder why polymerizing water-soluble monomer acrylic acid (AA) in water can form PAA nanogels but do not form bulk PAA hydrogels. To address this question, our group discovered and studied the acrylic acid-induced phase transition of

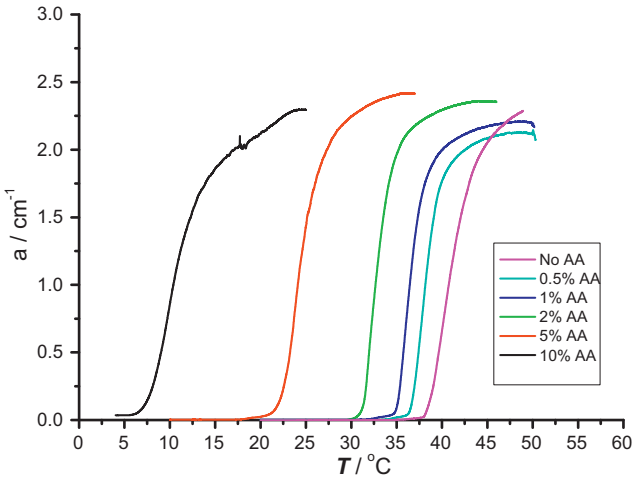

Fig. 1. Effect of AA concentration on the phase transition of HPC.

hydroxypropylcellulose (or HPC) at a temperature lower than 41 °C, a typical phase transition temperature of HPC. This new phenomena may be attributed to the formation of hydrogen bonds between AA and HPC. Just like HPC-PAA hydrogen bonding, AA–HPC hydrogen bonding reduces water–HPC hydrogen bonding, thus increasing inter-HPC hydrophobic interaction at a lower temperature.

To further understand the mechanism of the formation of PAA nanogels in the aqueous HPC solution, the acrylic acid (AA)-triggered temperature phase transition behavior has been studied. Specifically, the effect of acrylic acid (AA) concentration on the phase transition of 0.1 wt% hydroxypropylcellulose (HPC, DS 3.0, $M_w = 10^5$) is shown in Fig. 1. The phase transition temperature of HPC/AA aqueous solution was reduced from 38 °C to 32 °C while increasing the AA concentration from 0.5 wt% to 2.0 wt%. The decreasing phase transition temperature with increasing AA concentration is attributed to the formation of hydrogen bonding between the hydroxyl (–OH) group of HPC polymer and AA carboxyl group (–COOH). Such hydrogen bonding screens the access of water to the HPC polymer chains and reduces the solubility of the HPC in water, thus resulting in the increase of the hydrophobic association of the HPC interpolymers. The interpolymer hydrogen bonding between hydroypropylcellulose (HPC) and poly(acrylic acid) (PAA) demonstrated a stronger screening effect. For example, the phase transition temperature of 0.1 wt% HPC induced by 1 wt% PAA aqueous solution is at 25 °C, while the phase transition temperature of 0.1 wt% HPC triggered by 1 wt% AA aqueous solution is at 36 °C. The sharper decrease of the phase transition temperature induced by PAA may be due to much stronger inter-chain polymer hydrogen bonding between PAA–HPC compared with hydrogen bonding between AA–HPC. With a further increase of AA concentration up to 5 wt% and 10 wt%, the phase transition temperatures of HPC/AA aqueous solution were significantly reduced to 23 °C and 10 °C, respectively. The dramatic decrease of the phase transition temperature is attributed to a much stronger hydrophobic association of inter-HPC polymers induced by much more hydrogen bonding between HPC and AA due to an increase of AA concentration.

3.2. Effect of monomer AA concentration on PAA nanogels

In the HPC aqueous solution, AA molecules attach on the HPC polymer chains due to the hydrogen bonding between AA and HPC. As AA molecules polymerize to form PAA, PAA polymers form strong interpolymer hydrogen bonding with HPC, thus leading to a dramatic decrease in the phase transition temperature of HPC from 41 °C to below room temperature. The interpolymer

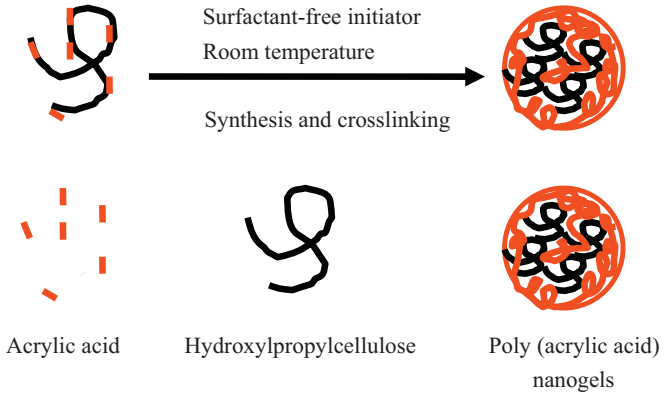

Scheme 1. Synthesis of PAA nanogels using HPC as template.

hydrogen bonding-induced phase transition causes the HPC polymer chains to collapse and form nanoparticles around room temperature. Therefore, PAA polymers attaching on HPC polymers form nanogels due to the formation of HPC nanogels as template, as shown in Scheme 1.

To study the synthesis of PAA nanogels in the HPC aqueous solution, the variation of AA concentrations listed in Table 1 at a HPC concentration of 0.4 wt% was conducted at 26 °C using 0.3 wt% BIS as crosslinker. After initiation, monomer AA absorbed on the HPC polymer chains polymerized immediately to form poly(acrylic acid) polymer chains. Because of the hydrogen bonding of PAA to HPC, HPC chains underwent phase transition and dehydrated to form a shrunken structure at 26 °C, much lower than 41 °C. Therefore, the PAA chains around HPC also dehydrated to form nanogels in the presence of crosslinker BIS. The critical turning point is the transition of the solution from transparent to light blue at a low pH (<3.5). However, we found that as AA was polymerized at pH = 5.0, 5.5, 6.0, respectively, the solution was still transparent. This means that no PAA nanogels formed under neutralized condition because no hydrogen bonding exists between HPC and PAA due to the ionization of AA and PAA.

The resulting PAA nanogels were measured by DLS measurement at 25 °C. The size and size distribution of surfactant-free PAA nanogels are shown in Fig. 2a. In Fig. 2, *x*-axis represents hydrodynamic diameter (D_h/nm) against *y*-axis indicating size distribution function $f_z(D_h)$. The results showed that an increasing AA concentration led to the bigger particle size of the resulting PAA nanogels, while the size distribution became slightly narrower. At a HPC concentration of 0.4 wt%, a higher AA concentration may form a higher concentration of PAA around HPC, thus leading to a large nanogel size at the ionized state due to static repulsion of the ionized PAA. Meanwhile, HPC chains can quickly dehydrate to form the nucleus of the nanogels when a higher AA concentration polymerizes to form PAA polymer chains. The fast formation of the shrunken HPC/PAA nanogels would be the reason for forming narrower size distribution of PAA nanogels. In the presence of 0.05 wt% SDS concentration, the effect of AA on the size and size distribution of the resulting PAA nanogels is shown in Fig. 2b. The size of the resulting

Table 1
Size and size distribution of PAA nanogels synthesized with varying AA concentration at 0.3 wt% BIS and 0.4 wt% HPC.

Surfactant-free				0.05 wt% SDS			
Sample	AA (wt%)	D_h (nm)	PDI	Sample	AA (wt%)	D_h (nm)	PDI
1	0.4	99.8	0.282	5	0.4	59.0	0.258
2	0.5	128.5	0.281	6	0.5	69.2	0.253
3	0.6	177.7	0.234	7	0.6	80.9	0.233
4	2	236.1	0.226	8	2	135.7	0.179

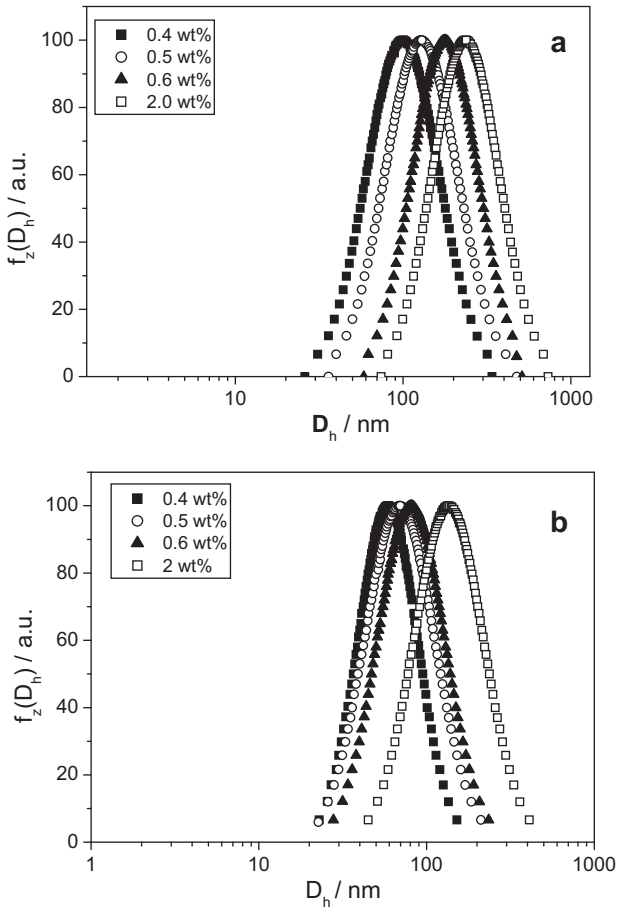

Fig. 2. (a) Effect of AA concentration on the size and size distribution of PAA nanogels without surfactant SDS. (b) Effect of AA concentration on the size and size distribution of PAA nanogels with 0.05 wt% surfactant SDS.

PAA nanogels increased with increasing AA monomer concentration and the size distribution of the PAA nanogels made with a higher AA concentration became narrower (Fig. 2b). As compared to the surfactant-free PAA nanogels, the PAA nanogels in the presence of 0.05 wt% SDS demonstrated much smaller particle sizes and more uniform size distribution.

TEM and AFM of PAA nanogels made with the formulation 0.4 wt% HPC, 0.4 wt% AA, and 0.3 wt% BIS are shown in Fig. 3a and b, respectively. From the TEM image, PAA nanogels showed a spherical shape and little aggregation and the average diameter of about 100 nm, while the average size of PAA nanogels characterized by DLS was about 178 nm in diameter. The size reduction in TEM is due to the collapse of the nanogels, while the size in AFM is about 165 nm close to the size of 178 nm at the swollen state.

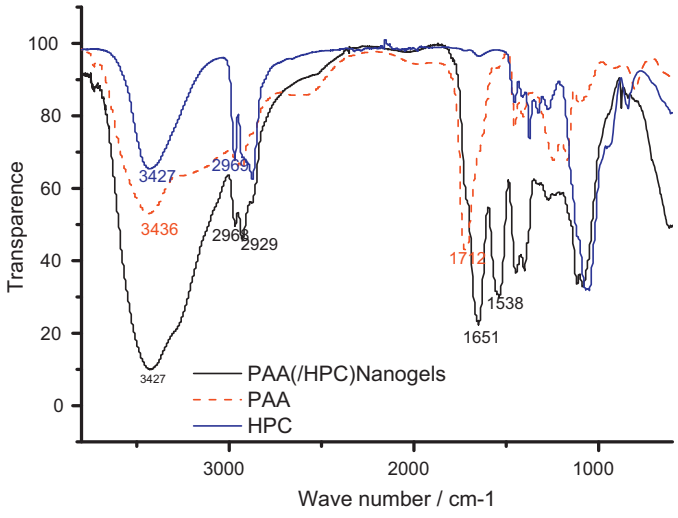

Fig. 4. FTIR spectra of HPC, PAA, and PAA nanogels containing HPC.

3.3. FTIR spectra of HPC, PAA, PAA(/HPC) nanogels

FTIR spectra of HPC, PAA, and PAA(/HPC) nanogels are given in Fig. 4. The absorption band at 3427 cm^{-1} showed that the hydroxyl group existed in the deprotonated PAA nanogels at pH = 6.3. Because no hydrogen bonding exists between the ionized PAA and HPC, the absorption peak at 3427 cm^{-1} corresponds to the hydroxyl group of HPC embedded in the PAA nanogels. For pure PAA, the absorption band of carboxyl groups at 1717 cm^{-1} can be observed. However, due to the ionization of the carboxyl group of PAA nanogel, the absorption bands at 1651 and 1538 cm^{-1} are attributed to carbonyl groups and carboxylate ions, respectively (Hu et al., 2002; Nurkeeva et al., 2004), while the typical absorption peak at 1717 cm^{-1} disappeared due to the conversion of carboxyl groups to carboxylate ions. The FTIR spectrum of the deprotonated PAA nanogels indicates the formation of the semi-interpenetrating structure of HPC with chemically crosslinked PAA nanogel networks.

3.4. Effect of HPC concentration on PAA nanogels

HPC as a template polymer plays a vital role in the synthesis of PAA nanogels. To study the effect of HPC concentration, the polymerization systems with four different HPC concentrations of 0.1 wt%, 0.2 wt%, 0.4 wt%, and 0.5 wt% were conducted at 2 wt%

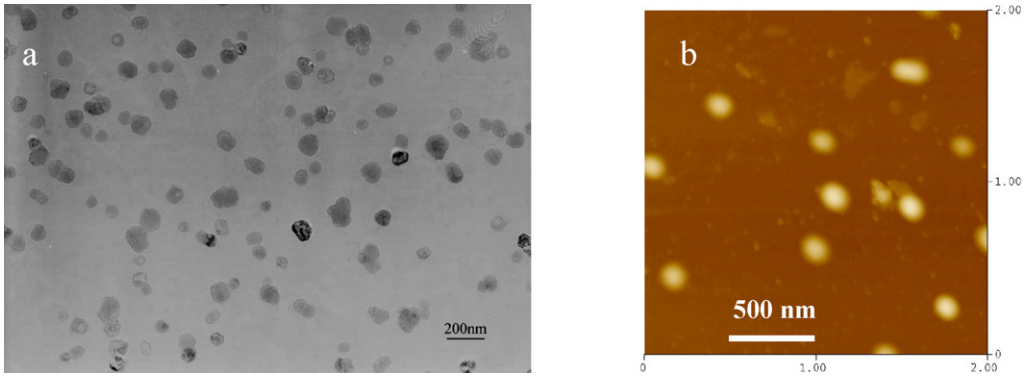

Fig. 3. TEM (a) and AFM (b) micrographies of PAA nanogels crosslinked with BIS.

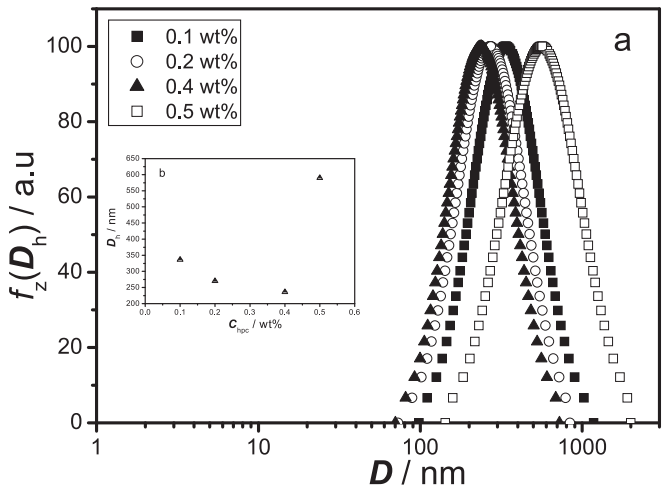

Fig. 5. (a) Effect of HPC concentration on size and size distribution of PAA nanogels. (b) Variation of PAA nanogel size synthesized with different HPC concentrations.

AA and 0.3 wt% BIS. The size and size distribution of the resulting PAA nanogels in varying HPC concentration are shown in Fig. 5. The results showed that with increasing HPC concentration from 0.1 wt% to 0.4 wt%, the size of PAA nanogels was reduced. But it did not mean that the higher HPC concentration, the smaller PAA nanogels. As the HPC concentration increased up to 0.5 wt%, the nanogels grew much larger. Interestingly, the size distributions of all the resulting PAA nanogels were only slightly different from each other.

Furthermore, the solution with 0.4 wt% HPC became light blue about 25 min after the polymerization was initiated at 26 °C. The respective solutions with 0.1 wt% HPC and 0.2 wt% HPC took a longer time to turn blue than the solution with 0.4 wt% HPC after initiating polymerization. It is reasonable that a higher HPC concentration easily leads to stronger hydrophobic association induced by PAA polymer chains. As HPC concentration further increased up to 0.5 wt%, the flocculation quickly occurred after polymerization without the deprotonation of PAA nanogels. But the deprotonated PAA nanogels were very stable due to the electrostatic repulsion of the ionic PAA nanogels.

3.5. Effect of crosslinkers on PAA nanogels

For comparison of the effect of crosslinkers on the synthesis of PAA nanogels, a set of experiments were conducted with 0.4 wt% AA and 0.4 wt% HPC at 26 °C using two kinds of crosslinkers (BIS and PEGDA). The effect of BIS concentrations of 0.05, 0.1, 0.2, 0.3 wt% on the size and size distribution of PAA nanogels is shown in Fig. 6a. The effect of PEGDA concentrations of 0.4, 1.0, 1.2, 1.6 wt% is shown in Fig. 6b. The results of PAA nanogel size and size distribution are listed in Table 2.

The particle size was reduced with an increase of BIS concentration, with the particle size being 99.8 nm at a concentration of 0.3 wt% BIS as shown in Table 2, whereas the size distribution became broader. Concerning the mechanism of PAA particle formation, the particle nucleation largely depends on the insolubility and hydrophobicity of the polymer chains. This would be understood by noting that the stronger hydrophobic feature of BIS segments at the higher concentration could enhance the insolubility of PAA nanogels. And the size distribution became broader due to the coalescence of the PAA nucleation with higher crosslinker concentration.

Poly(ethylene glycol) (PEG) is a well-known biocompatible polymer that has found a variety of biomedical applications (Knop, Hoogenboom, Fischer, & Schubert, 2010). PEG has demonstrated

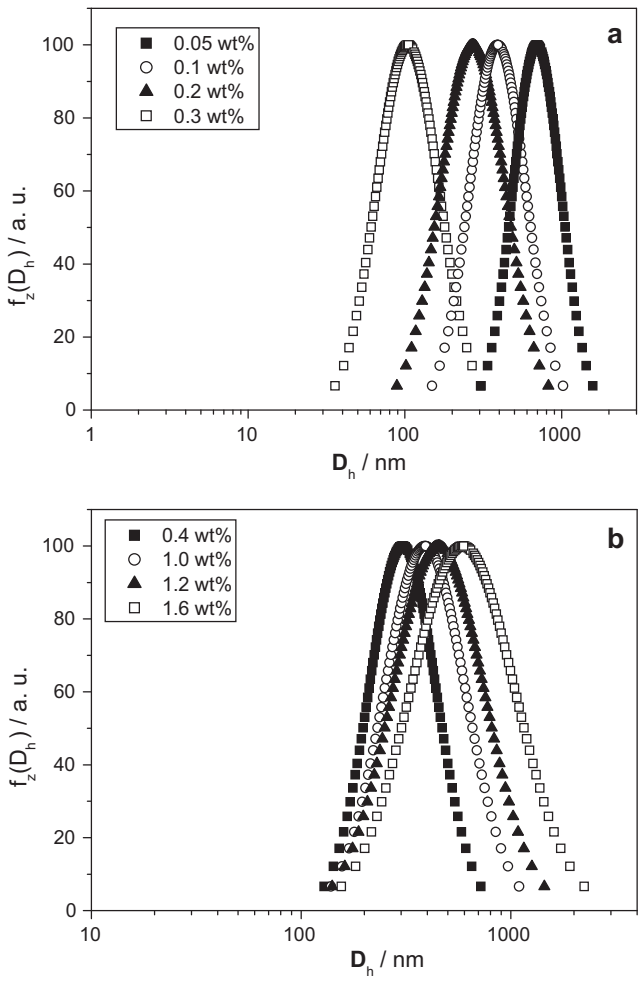

Fig. 6. (a) Effect of crosslinker BIS concentration on PAA nanogels. (b) Effect of crosslinker PEGDA concentration on size and size distribution of PAA nanogels.

the stealth behavior in coating nanoparticles for disease diagnosis and treatment and by coating nanoparticles can prevent their aggregation by steric stability. Gref et al. (1994) studied the pharmacokinetics of poly(lactic-co-glycolic acid) nanoparticles with PEG surface coverage and found that less than 30% of the 20 kDa PEG-coated nanoparticles were removed by the liver up to 2 h after injection, while most of the uncoated particles were captured by the liver only several minutes after injection. Recently, PEG-coated polymer nanoparticles for cancer magnetic resonance imaging and drug delivery system have been deeply studied (Kang, Josephson, Petrovsky, Weissleder, & Bogdanov, 2002; Laurent et al., 2008; Lee et al., 2006; Moffat et al., 2003). Until now, PEG is only one synthetic polymer in the market for all PEGylated drug delivery systems (Allen & Cullis, 2004).

In contrast to the BIS-crosslinked PAA nanogels, the PEGDA-crosslinked PAA nanogels exhibited increasing particle size and broader size distribution. Since PEG segments are much more hydrophilic than BIS, the increasing amount of crosslinker PEGDA can result in increased hydrophilicity of the PAA nanogels. The more hydrophilic character of polymer segments would lead to the increased size distribution. Furthermore, by incorporation of the hydrophilic PEG chains, the system enjoyed the bigger nucleus. Thus, it can be easily understood why PAA nanogels with PEG exhibited larger size than those with BIS. In agreement with the variations of PAA-BIS samples, the broader size distribution could be attributed to the coalescence of the PAA nucleation with higher

Table 2
Effects of crosslinker effects on size and size distribution of PAA nanogels.

	BIS concentration (wt%)				PEG concentration (wt%)			
Sample	1	2	3	4	5	6	7	8
Crosslinker	0.05	0.1	0.2	0.3	0.4	1.0	1.2	1.6
D_h (nm)	694.5	389.9	270.5	99.8	304.6	389.7	450.8	590
Polydispersity	0.132	0.186	0.256	0.281	0.146	0.217	0.284	0.388

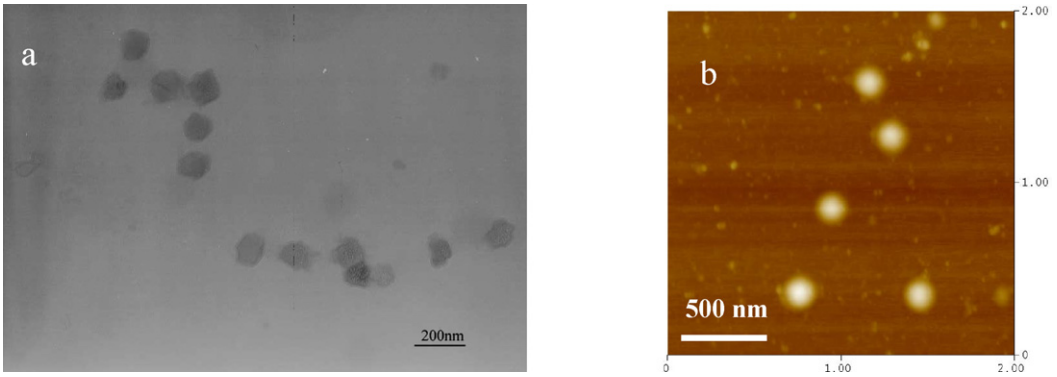

Fig. 7. TEM (a) and AFM (b) micrographies of PAA nanogels crosslinked with PEGDA.

crosslinker concentration and low charge density at the particle surface.

TEM and AFM of PAA nanogels with 0.4 wt% AA, 0.4 wt% HPC, and 0.4% PEGDA polymerized at 26 °C are shown in Fig. 7a and b, respectively. From the TEM Image (Fig. 7a), PAA nanogels showed a spherical shape and little aggregation and the average diameter of about 120 nm, while the average size of PAA nanogels characterized by DLS was about 305 nm in diameter. The size reduction in TEM is due to the collapse of the nanogels. The size in AFM is about 208 nm smaller than the size of 305 nm at the swollen state due to the evaporation of water out of PEGDA-crosslinked PAA nanogels observed with AFM.

4. Conclusions

Acrylic acid (AA) triggered phase transition of hydroxypropylcellulose (HPC) in aqueous media occurred at a decreasing temperature with an increasing concentration of AA due to hydrogen bonding between AA and HPC. As acrylic acids (or AAs) attached to the HPC were polymerized to form PAA, PAA have much stronger hydrogen bonding with HPC, still attaching on the HPC polymer chains. The PAA/HPC interpolymer hydrogen bonding can significantly decrease the phase transition temperature of the HPC, even down to around room temperature at which HPC collapsed to form nanogels. Thus, PAA collapsed with HPC to form nanogels in aqueous media without any surfactant. The analytical results showed that the PAA nanogels synthesized with HPC template demonstrated the narrow size distribution with the diameters ranging from 60 nm to 600 nm. The size and size distribution were controlled by monomer AA concentration, HPC concentration, and crosslinker kind and concentration. At the 0.4% HPC and 0.3% BIS, the size of the resulting PAA nanogels was increased as AA concentration increased from 0.4% to 2.0%. With the addition of 0.05% SDS, the nanogel size was reduced to around half of the nanogel size at the same formulation without surfactant. At 2% AA and 0.3% BIS, the nanogel size was reduced with increasing HPC concentration from 0.1% to 0.4%, while the nanogel size reversely increased at 0.5% HPC. The increasing nanogel size may be due to the instability of the resulting nanogel at a higher HPC concentration. The effect of crosslinker depended on its polarity. As increasing BIS concentration, the nanogel size was reduced, while the nanogel size was increased with an increasing concentration of hydrophilic PEGDA from 0.4% to 1.2%. With the help of hydrogen bonding interaction, the HPC-templated synthesis of surfactant-free PAA nanogels will open an “green” avenue to the formation of hydrophilic nanogels directly in aqueous media. Moreover, PEG-based PAA nanogels can hold promise for the development of nontoxic, biocompatible nanodevices that are easily functionalized with the carboxylic acid group of the PAA nanogels. The deprotonated PAA nanogels with carboxylic ions can absorb cationic metals and oxide or reduce inside individual nanogel to form novel hybrid nanomaterials.

Acknowledgment

This research was financially supported by Shanghai Municipality Research Project (No. 09520709600).

References

Allen, T. M., & Cullis, P. R. (2004). Drug delivery systems: Entering the mainstream. *Science*, *303*, 1818–1822.
Chang, C., & Zhang, L. (2011). Cellulose-based hydrogels: Present status and application prospects. *Carbohydrate Polymers*, *84*, 40–53.
Chu, B. (1991). *Laser light scattering* (2nd ed.). New York: Academic Press.
Gref, R., Minamitake, Y., Peracchia, M. T., Trubetskoy, V., Torchilin, V., & Langer, R. (1994). Biodegradable long-circulating polymeric nanospheres. *Science*, *263*, 1600–1603.
Hu, X., Tong, Z., & Lyon, L. A. (2010). Multicompartment core/shell microgels. *Journal of the American Chemical Society*, *132*, 11470–11472.
Hu, Y., Jiang, X., Ding, Y., Ge, H., Yuan, Y., & Yang, C. (2002). Synthesis and characterization of chitosan–poly(acrylic acid) nanoparticles. *Biomaterials*, *23*, 3193–3201.
Kang, H. W., Josephson, Petrovsky, L. A., Weissleder, R., & Bogdanov, A. J. (2002). Magnetic resonance imaging of inducible E-selectin expression in human endothelial cell culture. *Bioconjugate Chemistry*, *13*, 122–127.
Khemtong, C., Kessinger, C., & Gao, J. (2009). Polymeric nanomedicine for cancer MR imaging and drug delivery. *Chemical Communications*, *45*, 3497.
Kim, J., Singh, N., & Lyon, L. A. (2006). Label-free biosensing with hydrogel microlenses. *Angewandte Chemie International Edition*, *45*, 1446–1449.
Knop, K., Hoogenboom, Fischer, D., & Schubert, U. S. (2010). Poly(ethylene glycol) in drug delivery: Pros and cons as well as potential alternatives. *Angewandte Chemie International Edition*, *49*, 6288–6308.
Kriwet, B., Walter, E., & Kissel, T. (1998). Synthesis of bioadhesive poly(acrylic acid) nano- and microparticles using an inverse emulsion polymerization method for the entrapment of hydrophilic drug candidates. *Journal of Controlled Release*, *56*, 149–158.

Landfester, K., Willert, M., & Antonietti, M. (2000). Preparation of polymer particles in nonaqueous direct and inverse miniemulsions. *Macromolecules*, *33*, 2370–2376.
Laurent, S., Forge, D., Port, M., Roch, A., Robic, C., Elst, L. V., et al. (2008). Magnetic iron oxide nanoparticles: Synthesis, stabilization, vectorization, physicochemical characterizations, and biological applications. *Chemical Reviews*, *108*, 2064–2110.
Lee, H., Lee, E., Kim, D. K., Jang, N. K., Jeong, Y. Y., & Jon, S. (2006). Antibiofouling polymer-coated superparamagnetic iron oxide nanoparticles as potential magnetic resonance contrast agents for in vivo cancer imaging. *Journal of the American Chemical Society*, *128*, 7383–7389.
Lee, H., Yu, M. K., Park, S., Moon, S., Min, J. J., Jeong, Y. Y., et al. (2007). Thermally cross-linked superparamagnetic iron oxide nanoparticles: Synthesis and application as a dual imaging probe for cancer in vivo. *Journal of the American Chemical Society*, *129*, 12739–12745.
Lu, X., Hu, Z., & Gao, J. (2000). Synthesis and light scattering study of hydroxypropyl cellulose microgels. *Macromolecules*, *33*, 8698–8702.
Lu, X., Hu, Z., & Schwartz, J. (2002). Phase transition behavior of hydroxypropylcellulose under interpolymer complexation with poly(acrylic acid). *Macromolecules*, *35*, 9164–9168.
Moffat, B. A., Reddy, G. R., McConville, P., Hall, D. E., Cbenevert, T. L., Kopelman, R. R., et al. (2003). A novel polyacrylamide magnetic nanoparticle contrast agent for molecular imaging using MRI. *Molecular Imaging*, *2*, 324–332.
Nurkeeva, Z. S., Khutoryanskiy, V. V., Mun, G. A., Bitekenova, A. B., Kadlubowski, S., Shilina, Y. A., et al. (2004). Interpolymer complexes of poly(acrylic acid) nanogels with some non-ionic polymers in aqueous solutions. *Colloids and Surfaces A: Physicochemical and Engineering Aspects*, *236*, 141–146.
Peer, D., Karp, J. M., Hong, J. S., Farokhzad, O. C., Margalit, R., & Langer, R. (2007). Nanocarriers: Emerging platforms for cancer therapy. *Nature Nanotechnology*, *2*, 751–760.
Pelton, R. H. (2000). Temperature-sensitive aqueous microgels. *Advances in Colloid and Interface Science*, *85*, 1–33.
Pelton, R. H., & Chibante, P. (1986). Preparation of aqueous lattices with N-isopropylacrylamide. *Colloids and Surfaces*, *20*, 247–256.
Scherzinger, C., Lindner, P., Keerl, M., & Richtering, W. (2010). Cononsolvency of poly(N,N-diethylacrylamide) (PDEAAM) and poly(N-isopropylacrylamide) (PNIPAM) based microgels in water/methanol mixtures: Copolymer vs core–shell microgel. *Macromolecules*, *43*, 6829–6833.
Tabuchi, M., Ueda, M., Kaji, N., Yamasaki, Y., Nagasaki, Y., Yoshikawa, K., et al. (2004). Nanospheres for DNA separation chips. *Nature Biotechnology*, *22*, 337–340.
Uraki, Y., Imura, T., Kishimoto, T., & Ubukata, M. (2004). Body temperature-responsive gels derived from hydroxypropylcellulose bearing lignin. *Carbohydrate Polymers*, *58*, 123–130.
Wang, J., Gan, D., Lyon, L. A., & El-Sayed, M. A. (2001). Temperature-jump investigations of the kinetics of hydrogel nanoparticle volume phase transitions. *Journal of the American Chemical Society*, *123*, 11284–11289.
Wu, W., Shen, J., Banerjee, P., & Zhou, S. (2010). Hybrid micro-/nanogels for optical sensing and intracellular imaging. *Biomaterials*, *31*, 7555–7566.
Xu, X., Goponenko, A. V., & Asher, S. A. (2008). Polymerized polyHEMA photonic crystals: pH and ethanol sensor materials. *Journal of the American Chemical Society*, *130*, 3113–3119.
Yao, R., Xu, J., Lu, X., & Deng, S. (2011). Phase transition behavior of HPMC-AA and preparation of HPMC-PAA nanogels. *Journal of Nanomaterials*, 6 pages.
Yu, M. K., Jeong, Y. Y., Park, J., Park, S., Kim, J. W., Min, J. J., et al. (2008). Drug-loaded superparamagnetic iron oxide nanoparticles for combined cancer imaging and therapy in vivo. *Angewandte Chemie International Edition*, *47*, 5362–5365.
Zhang, J., Xu, S., & Kumacheva, E. (2004). Polymer microgels: Reactors for semiconductor, metal, and magnetic nanoparticles. *Journal of the American Chemical Society*, *126*, 7908–7914.